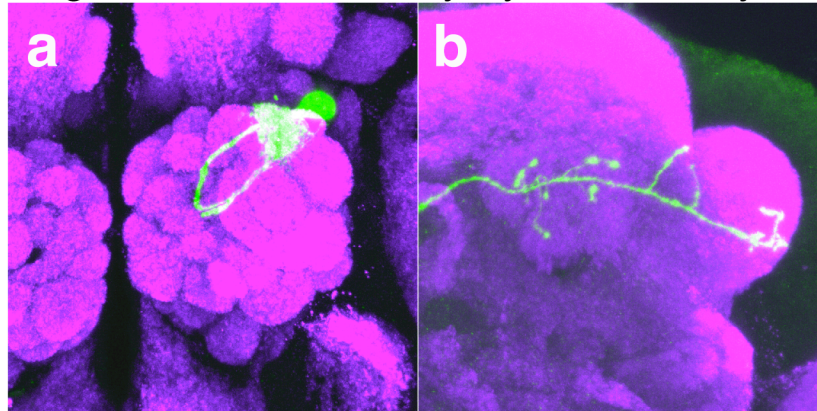
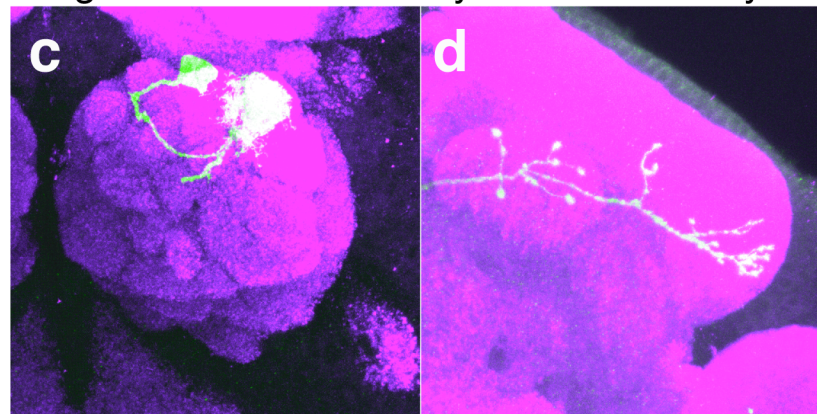


Supplementary Figure 1 Lack of axon terminal arborization in *team*^{-/-} PNs. Axon of *gars^{team/team}* PN clone occasionally reaches the lateral horn (n = 3/10), but their terminal arborization fails to elaborate. PN axon (green) is stained with anti-mouse CD8 antibody and presynaptic regions (magenta) are stained with nc82 antibody. Dotted circles indicate the calyx region of mushroom body (MB) and lateral horn (LH).

gars^{EX34/EX34} rescued by Cyto-GARS-Myc

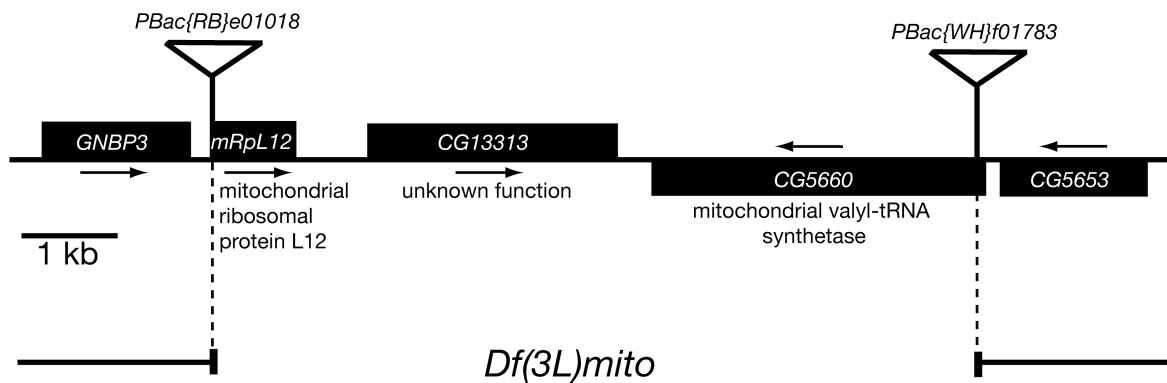


gars^{EX34/EX34} rescued by Mito-GARS-Myc



Supplementary Figure 2 MARCM rescue experiments of *gars*^{EX34/EX34} PN clone with either cytoplasmic or mitochondrial GARS. Post-mitotic expressions (*Gal4-GH146*) of either Cyto-GARS-Myc (a and b) or Mito-GARS-Myc (c and d) were able to rescue both dendritic and axonal phenotypes of *gars*^{EX34/EX34} PN clone. No differential rescuing capacity was detected. This is likely caused by leaky expression of Mito-GARS-Myc in the cytoplasm as was reported previously in yeast¹. Staining with nc82 and anti-mouse CD8 antibodies are shown in magenta and green, respectively.

1. Chang, K.J. & Wang, C.C. Translation initiation from a naturally occurring non-AUG codon in *Saccharomyces cerevisiae*. *J Biol Chem* **279**, 13778-85 (2004).



Supplementary Figure 3 Generation of *Df(3L)mito*. The genomic region between *PBac{RB}e01018* and *PBac{WH}f01783* was deleted according to Parks *et al*¹. The genomic deletion was confirmed by genomic PCR and lethal complementation test. Three genes including two genes related to mitochondrial protein translation should be completely disrupted in *Df(3L)mito* deletion stock.

1. Parks, A.L. et al. Systematic generation of high-resolution deletion coverage of the *Drosophila melanogaster* genome. *Nat Genet* **36**, 288-92 (2004).

Supplementary Methods

MARCM-based forward genetic screen

We used ethylmethane sulfonate (EMS) to mutagenize flies carrying FRT^{2A} and FRT^{82B} transgenes, which are sites for the FLP-mediated recombination in third chromosome left and right arms, respectively. Males carrying isogenized third chromosomes homozygous for FRT^{2A} , FRT^{82B} , $P[y+]$ were treated with 25 mM EMS. After establishing individual mutant stocks and confirming the lethality of mutations located on FRT -containing third chromosomes, we crossed these mutants to “MARCM-ready fly stock”. (For third chromosome left arm screen: $y w$, $hs-flp122$, $UAS-mCD8-GFP$; $Gal4-GH146$, $UAS-mCD8-GFP / CyO$; $tubP-Gal80$, $FRT^{2A} / TM3 Sb$. For third chromosome right arm screen: $y w$, $hs-flp122$, $UAS-mCD8-GFP$; $Gal4-GH146$, $UAS-mCD8-GFP / CyO$; FRT^{82B} , $tubP-Gal80 / TM3 Sb$.) We heat-shocked progenies of these crosses at 4–20 hr after larval hatching for 1 hr at 37°C. Then, we dissected out adult fly brains of the appropriate genotype and analyzed the PN dendritic and axonal projection patterns visualized by expression of mCD8-GFP in whole mount live brains under a compound fluorescence microscope.

Genetic mapping of *team* ($gars^{team}$) mutant

Genetic mapping for the causal gene of *team* was first performed with SNP-based recombination mappings¹. This mapping showed that the responsible mutation for the PN phenotypes in *team*^{-/-} MARCM clone is at a cytological location between 70D5 and 72C1. Next, we performed lethal complementation test with available deficiency lines within this candidate region, assuming *team* is homozygous lethal. $Df(3L)Brd12$, $Df(3L)Brd15$, $Df(3L)XG6$, $Df(3L)XG14$, $Df(3L)XG15$, $Df(3L)XG16$ failed to complement lethality of *team* whereas $Df(3L)XG4$, $Df(3L)XG7$ complemented, suggesting that *team* chromosome maps within genomic region from 71A3 to 71B8 (~280 kb). Next, we utilized the mapping method measuring the recombination rate from genetically mapped P-element insertion site². Genetic distances from the *team* lethal mutation to P-element insertions; $GS3025$, $GS13002$, $GS9061$, $EP3609$ and $KG02744$ were 0.000, 0.050, 0.162, 0.407 and 0.262 cM, respectively, suggesting that the lethal mutation is around the genomic region from 71B3 to 71B7 (~120 kb). Then, we collected

genomic DNA from embryos homozygous for *team* selected by single embryo PCR, and sequenced open reading frames, splicing acceptor and donor sites of all genes in this region. A missense mutation in *CG6778*, *glycyl-tRNA synthetase* (*gars*) was confirmed three times by sequencing independent PCR products amplified from genomic DNA homozygous or heterozygous for *team* and parental alleles.

Fly stocks

We used the following additional mutants to assess the function of protein translation in neuronal morphogenesis: *P{EPgy2}Aats-gly^{EY09021}*, *P{PZ}Aats-gln⁰⁵⁴⁶¹*, *tko³* (ref.³), *wars⁴* (ref.⁴), *P{tko^{25t-H85L}}*³². To generate *gars* null mutant, *gars^{EX34}*, imprecise excision of *P{EPgy2}Aats-gly^{EY09021}* was performed using the *delta2-3* transposase. Loss of the *mini-white* transgene marker was used as an initial screen, and the deleted genomic region was confirmed by genomic PCR. *Df(3L)mito* was generated according to the method described by Parks *et al*⁵. Genotypes used in this study are: (1) *gars* loss-of-function in PN (**Fig. 1c, d, g, h, 2d, e, 3e-h**): *y w, hs-FLP122, UAS-mCD8-GFP/UAS-syt-HA* or +; *Gal4-GH146, UAS-mCD8-GFP/+; gars^{team or EX34}, FRT^{2A} /tubP-GAL80, FRT^{2A}*. (2) *gars* loss-of-function in MB neuron (**Fig. 7f and g**): *y w, hs-FLP, UAS-mCD8-GFP/Y* or +; *UAS-mCD8-GFP/+; gars^{EX34}, FRT^{2A} /tubP-GAL80, FRT^{2A}; Gal4-OK107/+*. (3) *gars* rescue (**Fig. 2f, g and 8c-h**): *y w, hs-FLP122, UAS-mCD8-GFP; Gal4-GH146, UAS-mCD8-GFP/UAS-gars transgenes (various types); gars^{team or EX34}, FRT^{2A} /tubP-GAL80, FRT^{2A}*. (4) *gars* or *wars* loss-of-function in PN (**Fig. 5**): *y w, hs-FLP122, UAS-mCD8-GFP; Gal4-GH146, UAS-mCD8-GFP/+; FRT^{82B}, gars or wars/ FRT^{82B}, tubP-GAL80*. (5) *wars⁴* loss-of-function in MB neuron (**Fig. 7h and i**): *y w, hs-FLP, UAS-mCD8-GFP/Y* or +; *UAS-mCD8-GFP/+; FRT^{82B}, wars⁴/ FRT^{82B}, tubP-GAL80; Gal4-OK107/+*. (6) *tko³* loss-of-function in PN (**Fig. 6c-f**): *tko³, FRT^{19A}/y w, hs-FLP122, tubP-GAL80, FRT^{19A}; Gal4-GH146, UAS-mCD8-GFP/Gal4-GH146, UAS-mCD8-GFP*. (7) *tko³* loss-of-function in MB neuron (**Fig. 7j and k**): *tko³, FRT^{19A}/y w, hs-FLP, tubP-GAL80, FRT^{19A}; UAS-mCD8-GFP/+; Gal4-OK107/+*. (8) *Df(3L)mito* MARCM analysis (images not shown, quantified in **Fig. 6g and h**): *y w, hs-FLP122, UAS-mCD8-GFP; Gal4-GH146, UAS-mCD8-GFP/+; Df(3L)mito, FRT^{2A}/tubP-GAL80, FRT^{2A}*. (6) *Drosophila* GARS-Myc localization in PN (**Fig. 4a, c, e**): *y w; Gal4-Mz19, UAS-mCD8-GFP / UAS-(full, cyto or*

mito)-gars-myc. (**Fig. 4g and h**): *y w; Gal4-Mz19 / UAS-full-gars-myc; UAS-mitoGFP / +*.

Immunostaining

Fixation, immunostaining, and imaging were carried out as described⁶. Additional antibodies used in this study were anti-HA (12CA5), 1:1000; rabbit anti-GFP, 1:500 (Molecular Probe); rat anti-DN-Cadherin, 1:30; mouse anti-Myc (9E10), 1:250 (Developmental Studies Hybridoma Bank at the University of Iowa). Triple immunofluorescent stainings with anti-mouse CD8 (rat), anti-HA (mouse), and nc82 (mouse) antibodies were carried out with Zenon Alexa Fluo 647 mouse IgG1 labeling kit (Molecular Probe). mCD8-GFP was used primarily to visualize mutant neurons as it is an extremely stable protein (e.g. ORN axons and terminals separated from cell bodies for 50 days still retain mCD8-GFP staining, see MacDonald *et al.*⁷).

Transfection and MitoTracker staining

Cos-7 cells were cultured and transfected by using Lipofectamine (BRL). For *Drosophila* GARS-myc localization, we co-transfected *UAS-gars-myc* and *pSN3* vector that expresses GAL4 under control of CA promoter in Cos-7 cells. For human GARS-Myc localization, we transfected *pcDNA3-human-gars-myc* into Cos-7 cells. For MitoTracker staining and immunostaining, transfected Cos-7 cells were incubated with DMEM culture medium containing 200 nM of MitoTracker red CMXRos (Invitrogen) for 30 min before fixation. After fixation with 4% paraformaldehyde/PBS, cells were stained with mouse anti-Myc (9E10) at 1:250 dilution (Developmental Studies Hybridoma Bank at the University of Iowa).

1. Berger, J. et al. Genetic mapping with SNP markers in *Drosophila*. *Nat Genet* **29**, 475-81 (2001).
2. Zhai, R.G. et al. Mapping *Drosophila* mutations with molecularly defined P element insertions. *Proc Natl Acad Sci U S A* **100**, 10860-5 (2003).
3. Toivonen, J.M. et al. Technical knockout, a *Drosophila* model of mitochondrial deafness. *Genetics* **159**, 241-54 (2001).
4. Sessaiah, P. & Andrew, D.J. WRS-85D: A tryptophanyl-tRNA synthetase expressed

to high levels in the developing *Drosophila* salivary gland. *Mol Biol Cell* **10**, 1595-608 (1999).

5. Parks, A.L. et al. Systematic generation of high-resolution deletion coverage of the *Drosophila melanogaster* genome. *Nat Genet* **36**, 288-92 (2004).
6. Lee, T. & Luo, L. Mosaic analysis with a repressible cell marker for studies of gene function in neuronal morphogenesis. *Neuron* **22**, 451-61 (1999).
7. Macdonald, J.M. et al. The *Drosophila* cell corpse engulfment receptor draper mediates glial clearance of severed axons. *Neuron* **50**, 869-81 (2006).